

Plasmon dispersion and electron heating in a drifting two-dimensional electron gas

A. S. Bhatti, D. Richards, and H. P. Hughes

Optoelectronics Group, Cavendish Laboratory, Madingley Road, Cambridge CB3 0HE, United Kingdom

D. A. Ritchie, J. E. F. Frost, and G. A. C. Jones

MBE Group, Cavendish Laboratory, Madingley Road, Cambridge CB3 0HE, United Kingdom

(Received 19 July 1994)

We present Raman-scattering and photoluminescence measurements on a laterally drifting two-dimensional electron gas (2DEG) formed at a GaAs-Al_{0.3}Ga_{0.7}As heterojunction. The backscattering geometry employed allows both the direction, parallel, antiparallel, or perpendicular to the drift direction, and magnitude of the in-plane scattering wave vector to be varied. For a fixed wave vector the drift current produces a Doppler shift and broadening of the intrasubband plasmon Raman peak. For small drift velocities the energy shift is linear, and in opposite directions for the Stokes and anti-Stokes spectra, but becomes nonlinear for large drift velocities, and in the same direction in both cases. This change in behavior is ascribed to increasing carrier density with drift. Single-particle relaxation times were determined from the broadening of the plasmon Raman peaks. The ratio of the intensities of the Stokes and anti-Stokes plasmon peaks provides an estimate of the 2DEG temperature under drift conditions; this increased considerably with drift current, as confirmed by the high-energy tail of the band-gap photoluminescence from the 2DEG.

INTRODUCTION

A two-dimensional electron gas (2DEG) drifting under the influence of an in-plane electric field is of both physical and technological interest. The potential device applications of using high mobility heterostructures and/or superlattices as radiation sources and amplifiers based on current driven plasma instabilities have raised interest in the study of drifting 2DEG's.¹⁻⁶ Theoretical studies have shown that plasmon instabilities can occur for drift velocities equal to or larger than the 2DEG Fermi velocity, v_F (of the order of 10^7 cm s⁻¹), although such conditions have been shown to be very difficult to achieve experimentally in GaAs/Al_xGa_{1-x}As systems.^{7,8} The study of drifting 2DEG's in a HEMT (high electron mobility transistor) is also important in understanding electric-field-induced changes in the electron energy distribution, the various scattering mechanisms, and the saturation of the drift velocity at high fields.

Inelastic light scattering is a very powerful, contactless technique for studying electronic excitations, such as single-particle excitations or plasmons in 2DEG's.^{9,10} In this paper, the effects of electron drift, induced by an in-plane electric field, on the plasmon modes of the 2DEG are studied using Raman spectroscopy, providing information on the Doppler shift of the plasmon energy, the plasmon line shapes (and hence the single-particle relaxation times) and the temperature of the 2DEG.

In the Raman-scattering process, photons are scattered by excitations such as plasmons conserving both energy and momentum parallel to the sample surface, i.e., in the plane of the 2DEG. Excitations of wave vector $+\mathbf{q}_{\text{ex}}$ and energy $+\hbar\omega_{\text{ex}}$ are created in Stokes (S) scattering, whereas excitations of wave vector $-\mathbf{q}_{\text{ex}}$ and energy

$-\hbar\omega_{\text{ex}}$ are annihilated in anti-Stokes (AS) scattering, so the scattered light frequencies ω_s and wave vectors \mathbf{q}_s , both of which depend on the scattering geometry and are directly determined experimentally, are given by $\omega_s = \omega_i \pm \omega_{\text{ex}}$ and $\mathbf{q}_s = \mathbf{q}_i \pm \mathbf{q}_{\text{ex}}$. Both Stokes and anti-Stokes spectra can be simultaneously probed in a single Raman experiment.

For a drifting 2DEG a Doppler-type shift in the plasmon energy is expected. For drift velocities $v_d \ll v_F$ the energy ω of a plasmon is given by¹¹

$$\omega = \omega_p + \mathbf{q} \cdot \mathbf{v}_d, \quad (1)$$

where ω_p is the energy for zero drift, \mathbf{q} the plasmon wave vector, and v_d the drift velocity of the 2DEG. Such Doppler shifts have been observed using far-infrared (FIR) transmission spectroscopy,^{11,12} for which a metal grating is required to couple the radiation to the plasmon modes; the plasmon wave vector is fixed by the grating period so FIR studies are not possible over a continuous range of \mathbf{q} . The plasmon dispersion relation and the Doppler shift are also modified by the strong periodic screening by the coupling grating, which further compromises the uniformity of the applied drift field so that the simple picture of a spatially constant drift velocity no longer applies. Raman scattering, not requiring a grating, permits measurements of ω for a wide and continuous range of \mathbf{q} and v_d without these complications.¹³ In addition, measurement of both Stokes and anti-Stokes Raman scattering allows the observation of plasmons with wave vectors in opposite directions with respect to the drift. For example, if the Stokes Raman wave vector and hence the plasmon wave vector \mathbf{q} is parallel to the drift direction, then the plasmon observed in anti-Stokes

scattering has wave vector $-\mathbf{q}$, antiparallel to the drift.

Application of an in-plane electric field also results in heating of the 2DEG, which is of considerable theoretical and technological interest and has been studied extensively using band-gap photoluminescence (PL) measurements (e.g., Refs. 14, 17, and 18). Much work in this area has used steady currents to produce Joule heating in the 2DEG;¹⁵ the electrons gain energy from the applied field which is redistributed within the 2DEG through electron-electron or electron-phonon scattering. Electron-electron scattering processes have the effect of populating higher-energy states in the conduction band with electrons and producing a corresponding high-energy Boltzmann-like exponential tail to the PL spectra, characteristic of an electron temperature T_e greater than the lattice temperature T_L . On the other hand, electron-LO-phonon scattering tends to deplete the population of electrons above a threshold energy marked by a sharp cutoff in the PL spectra.¹⁶ Shah and Leite¹⁷ have measured the carrier temperature in GaAs (assuming $T_e = T_h$, the hole temperature) as a function of excitation power in a cw PL experiment by analyzing the high-energy tail of band to band emission. It should be noted, however, that PL from a 2DEG involves the radiative recombination of essentially *degenerate* electrons ($T_e \ll T_F$) with photoexcited holes, which themselves have an energy distribution with a characteristic temperature T_h ; it is, therefore, effectively the *hole* distribution that is probed and T_h that determines the high-energy PL tail. However, it may reasonably be assumed that the holes and electrons are in thermal equilibrium, and Southgate and co-workers using this method, have studied the heating of the electron distribution by an applied electric field.^{18,19} In addition, application of the Fermi-Dirac distribution function has also been shown to be a reliable way to extract the temperature of a drifting 2DEG.²⁰

The electron temperature can also be derived from the Raman-scattering measurements. The ratio of the Stokes and anti-Stokes plasmon intensities I_S and I_{AS} provides a direct estimate of the electron temperature T_e from²¹

$$\frac{I_{AS}}{I_S} = \exp \left[\frac{-\hbar\omega_p}{k_B T_e} \right], \quad (2)$$

where k_B is the Boltzmann constant.

EXPERIMENT

The sample studied was a standard HEMT structure, with layer sequence as follows: semi-insulating GaAs substrate, 0.67- μm GaAs buffer, 0.33- μm GaAs/AlAs superlattice (60 periods of 28- \AA GaAs/27- \AA AlAs thick layers), 1000- \AA GaAs active layer, 240- \AA $\text{Al}_{0.3}\text{Ga}_{0.7}\text{As}$ spacer, 480- \AA Si-doped $\text{Al}_{0.3}\text{Ga}_{0.7}\text{As}$, and 100- \AA GaAs capping layer. The electron mobility and carrier density obtained from Hall voltage measurements at a temperature of 1.6 K were $\mu = (2.2 \pm 0.2) \times 10^5 \text{ cm}^2 \text{ V}^{-1} \text{ s}^{-1}$ and $N_S = (2.1 \pm 0.2) \times 10^{11} \text{ cm}^{-2}$ in the dark, respectively, and $\mu = (3.0 \pm 0.3) \times 10^5 \text{ cm}^2 \text{ V}^{-1} \text{ s}^{-1}$ and $N_S = (2.5 \pm 0.3) \times 10^{11} \text{ cm}^{-2}$ after brief illumination by a red LED. The

active GaAs layer included a δ -doped Be layer ($2 \times 10^{10} \text{ cm}^{-2}$), 250 \AA from the active heterointerface, which confines the photohole produced in resonant electronic Raman scattering to the region near the heterointerface where the corresponding photoelectron is confined by the conduction-band bending; this enhances luminescence intensities²² and is believed also to account for the observed enhancement of electronic Raman scattering²³ in such heterojunction samples. A mesa etched area of the sample formed the drift channel of length 1000 μm and width 800 μm , with two primary Au/Ge/Ni ohmic contacts for applying the in-plane electric field, and two independent Au/Ge/Ni ohmic contacts, separated by 400 μm , on each side for measuring the voltage drop along the 2DEG.

Raman-scattering experiments were performed using a laser wavelength of 777.5 nm (near resonance with the GaAs E_0 band gap) and for a fixed momentum transfer (determined by the backscattering geometry) of $1.39 \times 10^5 \text{ cm}^{-1}$ except where stated explicitly otherwise. The laser power illumination at the sample surface was $\sim 30 \text{ mW}$ with a spot size of $\sim 350 \mu\text{m}$, and the lattice temperature was maintained at $\sim 7 \text{ K}$ on a cold finger in a He bath cryostat. The backscattering geometry and the rotatable sample mount allowed a range of momentum transfer \mathbf{q} to the 2DEG excitations, with direction parallel (P), antiparallel (AP), or perpendicular (\perp) to the drift velocity v_d , to be studied. The scattered light was energy dispersed using a DILOR XY triple grating spectrometer and detected with an intensified Si diode array. The selection rules for inelastic light scattering from the 2DEG allow plasmons and LO phonons to be observed when the incident and scattered polarizations are parallel (polarized scattering), and spin density excitations when incident and scattered polarizations are mutually perpendicular (depolarized scattering).⁹ Indeed a peak due to scattering from plasmons was observed in polarized Raman spectra, while no excitations were observed for depolarized scattering. Using the plasmon dispersion relation

$$\omega_p^2 = \frac{N_S e^2}{2\epsilon\epsilon_0 m^*} q \quad (3)$$

in two dimensions,²⁴ and taking into account the screening effects of the various layers in the sample that determine the effective dielectric constant ϵ ,²⁵ the 2DEG carrier density was estimated under zero drift conditions to be $N_S \approx 3.76 \times 10^{11} \text{ cm}^{-2}$.

Drift currents, constant to within $\pm 5\%$, up to 20 mA were generated by voltages applied to the end contacts of the drift channel; the current fluctuations arose from variations in the precise position of the laser spot on the drift channel, and the changes in the laser power density ($\pm 5\%$). I - V characteristics were found to be independent of the orientation of the sample to the laser beam, but were dependent on the bias direction for higher currents and were marked by a difference in the electron temperature for forward and reverse currents. The range of drift velocities probed was limited by the associated electron temperature rise which eventually broadened the band-

gap PL to higher energies sufficiently to obscure the plasmon Raman peak. Another limiting factor is the saturation of v_d at high electric field; v_d increases linearly with the applied electric field up to a certain critical value, above which it saturates as a consequence of the emission of LO phonons and intervalley scattering.^{8,26} Recent theoretical results for GaAs/ $\text{Al}_x\text{Ga}_{1-x}\text{As}$ quantum wells have shown that v_d should saturate at $\sim 2 \times 10^7 \text{ cm s}^{-1}$, independent of the zero-field mobility.⁸

RESULTS AND DISCUSSION

Figures 1(a)–(c) shows representative Stokes and anti-Stokes polarized Raman spectra for various drift currents for three orientations of wave-vector transfer with respect to the drift direction—parallel, antiparallel, and perpendicular—and Fig. 2 shows the variation with drift current of the plasmon energy observed in the parallel and antiparallel configurations.

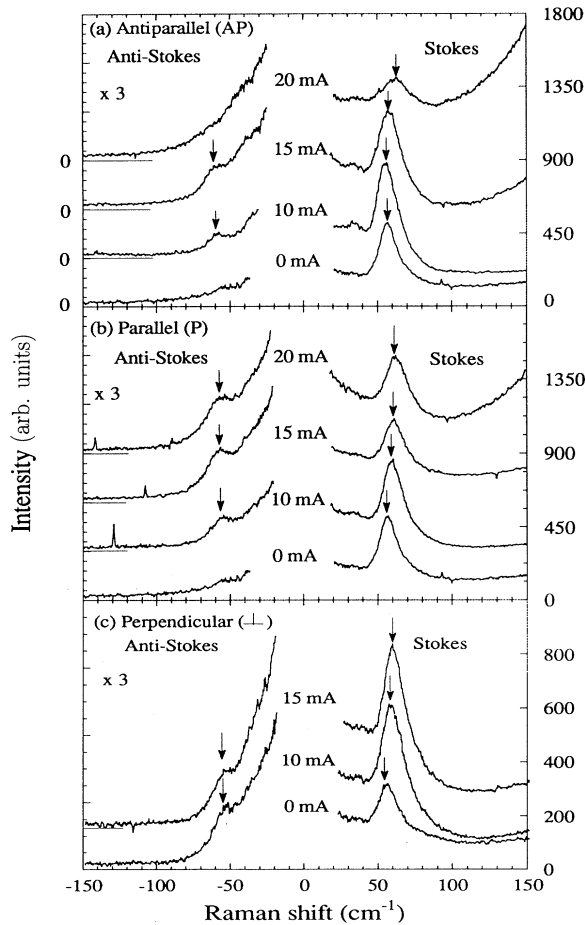


FIG. 1. Stokes and anti-Stokes polarized Raman spectra of a drifting 2DEG, with the Raman wave-vector transfer: (a) antiparallel (AP), (b) parallel (P), (c) perpendicular (\perp), to the drift velocity direction. Arrows indicate the intrasubband plasmon peaks. The Raman wave-vector transfer for P and AP is $1.39 \times 10^5 \text{ cm}^{-1}$ and for \perp is $1.35 \times 10^5 \text{ cm}^{-1}$. The spectra are displaced vertically for clarity.

For the antiparallel configuration (AP), the Stokes plasmon peak shifts toward lower energy as the drift current initially increases, as expected for a simple Doppler shift [Eq. (1)]. But for higher currents, it starts to shift to higher energy; the anti-Stokes plasmon peak develops with increasing current, growing in strength because of the increase in electronic temperature [Eq. (2)] and shifting to higher energy as expected from Eq. (1) since for anti-Stokes scattering the Raman wave vector $-\mathbf{q}$ is in the same direction as \mathbf{v}_d .

Similarly, for the parallel case (P), the Stokes plasmon energy shifts to higher energy, as expected from Eq. (1), since \mathbf{v}_d and the wave-vector transfer \mathbf{q} are in the same direction, but the rate of energy shift is greater than predicted. The anti-Stokes plasmon, for which \mathbf{v}_d and wave-vector transfer \mathbf{q} are in opposite directions, first shifts to lower energy as expected, and then to higher energy as N_S increases. A second peak at low energy (35 cm^{-1}) is also observed, the position of this peak is insensitive to current, and its origin is not clear.

It is clear from Fig. 2 that the anti-Stokes plasmon energy for the antiparallel case closely follows the Stokes plasmon energy for the parallel case, as expected since \mathbf{q} in both cases is parallel to \mathbf{v}_d . Likewise, the anti-Stokes plasmon for the parallel case closely follows the Stokes plasmon for the antiparallel case. The general increase of the means of the Stokes and anti-Stokes plasmon energies at the higher currents can be attributed to a current-induced increase in the 2DEG carrier density, and is confirmed by the perpendicular (\perp) case; no Doppler shift is expected, but again the Stokes and anti-Stokes plasmon energies increase with increasing current because of the increasing carrier density.

At this stage, a more exact comparison with the behavior expected from Eq. (1) can be made by calculating the drift velocity itself for each value of drift current. First, the modified carrier density N_S is determined at a particular current from the average of the Stokes and anti-Stokes plasmon energies, and the known 2DEG plasmon dispersion relation. Knowing N_S , \mathbf{v}_d can be obtained directly from the drift current, and is plotted as a function of a laterally applied electric field for both parallel and antiparallel cases in Fig. 3. It can be seen that \mathbf{v}_d increases linearly with field and starts to saturate at

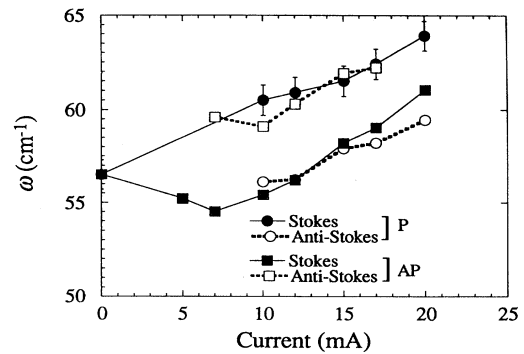


FIG. 2. Stokes (ω_S) and anti-Stokes (ω_{AS}) plasmon energies for the drifting 2DEG for P and AP configurations.

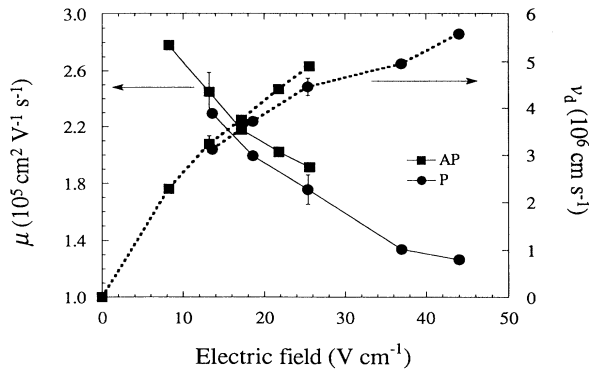


FIG. 3. Drift velocity v_d (dashed lines) and mobility μ (continuous line) for P and AP configurations as a function of in-plane applied electric field. v_d starts to saturate at higher electric fields.

higher applied fields as expected (e.g., Ref. 8). Knowing v_d , the electron mobility μ can also be obtained, and is shown in Fig. 3 plotted against the applied electric field; the reduction in μ from low field to high field is approximately 30%, comparable with the 30–50% found by others.^{13,27}

The Doppler shift in energy of the Stokes scattering for the three configurations are plotted against v_d in Fig. 4. The shift is determined by subtracting the Stokes plasmon energy from the average of the Stokes and anti-Stokes plasmon energies for a particular drift velocity. For lower v_d the Doppler splitting closely follows the expected behavior of $\pm qv_d$, but for higher v_d , it becomes almost constant. No Doppler shift between the Stokes and anti-Stokes scattering was found for the perpendicular configuration, as expected.

From these results, it can be seen that two factors contribute to the shift in plasmon energy—the increase in carrier density N_S (shown in Fig. 5, plotted against drift

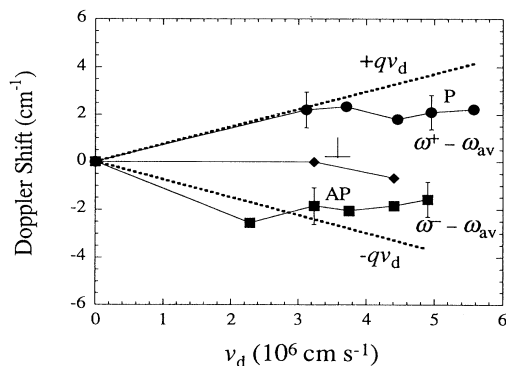


FIG. 4. Doppler shift of the Stokes plasmon energies for P , AP , and l versus v_d . The Doppler shift is obtained by subtracting the Stokes plasmon energy from the average of the Stokes and anti-Stokes plasmon energies. The shift is linear at small v_d and closely follows the expected behavior, $\pm qv_d$ (dashed lines). For higher v_d the shift saturates. No Doppler shift was found for the perpendicular configuration, as expected.

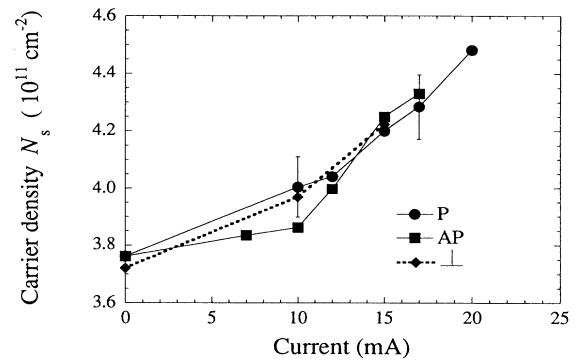


FIG. 5. Variation of the carrier density N_S , determined from the average of Stokes and anti-Stokes plasmon energies with drift current.

current), and the Doppler shift qv_d . For lower currents the energy shift is essentially the linear Doppler shift, while for higher currents, the major contribution comes from the increasing carrier density, as clearly demonstrated by the increase in plasmon energy with current when q and v_d are perpendicular. In thermal equilibrium, the carrier density is expected to increase with temperature. However, carrier densities calculated for a $\text{GaAs}/\text{Al}_x\text{Ga}_{1-x}\text{As}$ heterojunction showed a smaller increase with temperature than that observed in the present experiments (5% as compared to 19%).²⁸

For Raman-scattering measurements performed with a large spot size, covering the whole drift channel, with a lower incident laser power density ($\sim 8\text{--}10\text{ W cm}^{-2}$), a similar behavior of the Doppler shift is observed. The shift is linear for small drift velocities and saturates for higher drift velocities. An increase in carrier density is still observed with drift, although smaller than for the measurements with a small spot size.

Most single-particle relaxation times or quantum lifetimes reported in the literature are derived from Shubnikov–de Haas measurements.³⁰ The width of the Raman plasmon peak, however, gives a direct measure of the single-particle relaxation time τ_{sp} . The transport scattering time τ_{tr} for small-angle scattering can also be determined from the electron mobility μ . The ratio of these two scattering times usually indicates the dominant scattering mechanism at the heterojunction interface (for a detailed discussion on scattering mechanisms see Harang *et al.*²⁹ and Coleridge³⁰). τ_{tr} and τ_{sp} , and their ratio, are shown in Fig. 6 as functions of the drift current. The relaxation times decrease significantly with the increase of current, indicating the presence and strength of various scattering mechanisms. τ_{sp} for a nondrifting 2DEG is found to be 0.34 ± 0.03 ps, and decreases by about 30% at the maximum drift current [20 mA, Fig. 6(b)], suggesting an increase in electron-electron and electron-phonon interactions. The values of τ_{tr}/τ_{sp} are in the range 20–50, in good agreement with the values found experimentally and calculated theoretically by other authors for $\text{GaAs}/\text{Al}_x\text{Ga}_{1-x}\text{As}$ heterojunctions, considering remote ionized impurity scattering.^{31,32}

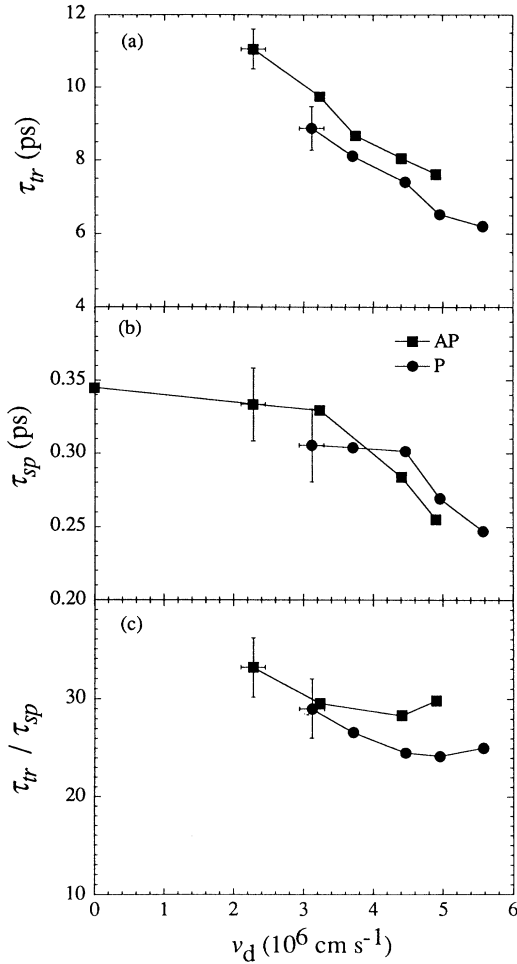


FIG. 6. (a) Transport scattering times (τ_{tr}) determined from the mobility; (b) single-particle scattering times (τ_{sp}) determined from the plasmon linewidth; (c) ratio of the two times (τ_{tr}/τ_{sp}); as functions of the drift velocity (for both AP and P).

In addition to the plasmon peak, the polarized Raman spectra also show a low-energy tail to the laser line, the intensity of which increases with current (see Fig. 1). The origin of this feature, which is clearly due to inelastic light scattering as it remains unchanged with different excitation energies, is not clear. One possible explanation of this continuum may be inelastic light scattering from acoustic phonons due to a partial breakdown of crystal momentum conservation in the growth direction; a similar structureless continuous spectrum close to the excitation line has been reported previously in multiple quantum well structures under strong magnetic fields (e.g., Ref. 33).

ELECTRON TEMPERATURE

GaAs/Ga_xAl_{1-x}As δ -doped heterostructures have been studied extensively using the PL technique.^{22,34} PL measurements on the drifting 2DEG were performed under the same illumination conditions as the Raman exper-

iments described above, and the results are shown in Fig. 7. The low- and high-energy peaks observed are assigned to the recombination of electrons with holes bound to acceptors (e -B), and with free holes (e -A), respectively. T_e , the temperature of the 2DEG, can be deduced from the exponential decay of the high-energy tail in the high-energy PL peak, assuming, as discussed above, that the electron and hole temperatures are equal. For the zero-drift case, T_e was 19 K, which is higher than the lattice temperature ($T_L = 7$ K) because of heating of the 2DEG by the laser. T_e was measured with different laser powers and, for the minimum laser power density (10 W cm^{-2}), was found to be 12 K. With increasing current the slope of the high-energy tail reflects the effect of electron heating, while the position of the PL peaks (e -A) and (e -B) are unchanged as T_e increases, indicating that the lattice temperature remains constant.

Figure 8 shows a comparison between the electron temperatures determined from the slope of the PL measurements, and from the ratio of the Stokes and anti-Stokes intensities of the plasmon peak in Raman scattering [Eq. (2)]. The rise in T_e is approximately linear with drift current, and the two techniques give broadly similar results. T_e determined from Raman scattering, however, is probably more reliable as this gives a direct measure of the temperature of the 2DEG, whereas PL is a complicated process, involving spatially direct and indirect transitions and electron and hole distributions functions, and the determination of temperature from the PL tail assumes that the recombining electrons and holes are in thermal equilibrium.

It can be seen that, for drift conditions, the electron temperature becomes quite high (up to 60 K)—comparable to the Fermi temperature ($T_F = 150$ K). The effect of electron temperature on the plasmon energy was investigated by performing calculations within the random-phase approximation (RPA), at temperatures comparable to T_F ; the results show an increase in the

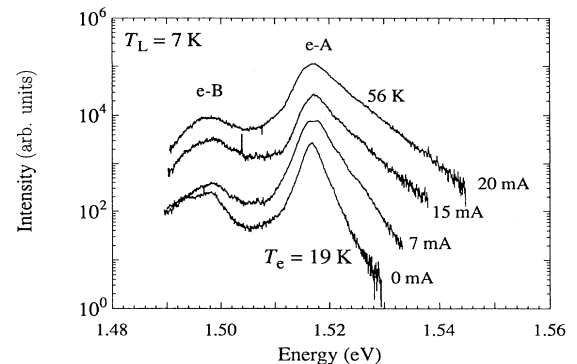


FIG. 7. Photoluminescence (PL) spectra for the anti-parallel (AP) configuration at various currents. (e -A) and (e -B) are the peaks due to recombination of electrons with free and bound holes, respectively. The spectra were obtained under the same conditions as the Raman-scattering experiments. The laser power density was 30 W cm^{-2} and the lattice temperature was 7 K. The spectra are displaced vertically for clarity.

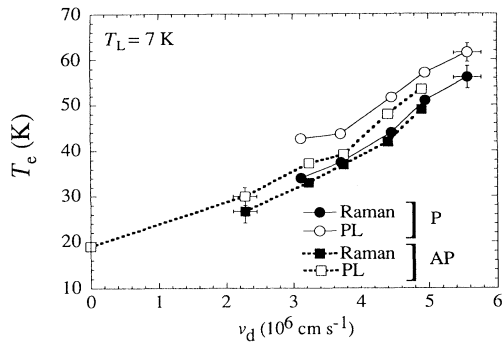


FIG. 8. Comparison of electron temperatures (T_e) obtained from the high-energy tail of the PL spectra and from the ratio of intensities of Stokes and anti-Stokes of Raman measurements. The increase in T_e with current is approximately linear, and both techniques are in broad agreement, although the Raman determination is expected to be more reliable.

plasmon energy with temperature, but the shifts are small (only $\sim 1 \text{ cm}^{-1}$) for the temperature range found experimentally, compared to the shift observed. The plasmon line shapes calculated in this manner were fitted for different single-particle relaxation times for fixed electron temperatures. The single-particle relaxation times obtained from the best fits were found to be consistent with the relaxation times determined from the experimental line shapes [see Fig. 6(b)]. The widths of the calculated plasmon peaks were found not to depend on electron temperature.

CONCLUSIONS

Both Stokes and anti-Stokes scattering from the plasmon of a drifting 2DEG have been observed. The ra-

tio of the Stokes and anti-Stokes plasmon intensities gave a measure of electron temperature, which was found to be consistent with the temperature determined from the measurements of the photoluminescence of the drifting 2DEG under the same conditions. The applied electrical field caused the electron temperature to rise considerably. The shift in the energy of the plasmon of the drifting 2DEG was found to be linear at small drift velocities, as predicted by theory for the Doppler shift of the plasmon, but a nonlinear behavior was observed at larger drift velocities, due to an increase in carrier density with drift. The anti-Stokes plasmon energy with the Raman wave vector antiparallel to the drift direction follows the Stokes plasmon energy for the parallel configuration, and similar behavior is observed for the other two configurations. No Doppler shift of the plasmon energy for the perpendicular configuration was observed. The single-particle scattering rate, determined from the widths of the plasmon peaks, increases with increasing drift of the 2DEG. Small-angle scattering times were determined from mobility measurements, and the ratio of the two scattering times was found to be consistent with values quoted by other authors. A low-energy background, the intensity of which was found to increase with current, is possibly due to inelastic light scattering by acoustic phonons, aided by a lack of translational symmetry in the growth direction.

ACKNOWLEDGMENTS

We thank L.C. Ó Súilleabháin for device fabrication and for helpful discussions and advice. The authors would like to thank D. J. Lovering for advice and technical assistance. This work was supported by the U.K. SERC. A.B. was supported by the Association of Commonwealth Universities, U.K. D.R. thanks St. John's College, Cambridge, for support.

- ¹J. Chen, K. Kempa, and P. Bakshi, *Phys. Rev. B* **38**, 10051 (1988).
- ²R. Gupta and B. K. Ridley, *Phys. Rev. B* **39**, 6208 (1989).
- ³A. V. Chaplik, *Surf. Sci. Rep.* **5**, 289 (1985).
- ⁴K. Kempa, *Appl. Phys. Lett.* **50**, 1185 (1987).
- ⁵P. Bakshi and K. Kempa, *Phys. Rev. B* **40**, 3430 (1989).
- ⁶K. Kempa, P. Bakshi, and H. Xie, *Phys. Rev. B* **48**, 9158 (1993).
- ⁷W. Masselink, *Semicond. Sci. Tech.* **4**, 503 (1989).
- ⁸L. S. Tan, S. J. Chua, and V. K. Arrora, *Phys. Rev. B* **47**, 13 868 (1993).
- ⁹G. Abstreiter, M. Cardona, and A. Pinczuk, in *Light Scattering in Solids IV*, edited by M. Cardona and G. Guntherodt (Springer, Heidelberg, 1984), p. 5.
- ¹⁰A. Pinczuk and G. Abstreiter, in *Light Scattering in Solids V*, edited by M. Cardona and G. Guntherodt (Springer, Heidelberg, 1988), p. 153.
- ¹¹H. P. Hughes, R. E. Tyson, L. C. Ó Súilleabháin, and R. J. Stuart, in *Proceedings of NATO Advanced Research Workshop on Negative Differential Resistance and Instabilities in 2-D Semiconductors*, edited by N. Balken, J. A. Vickers, and B. Ridley (Plenum, New York, 1993), p. 153.
- ¹²R. E. Tyson, R. J. Stuart, H. P. Hughes, J. E. F. Frost, D. A. Ritchie, G. A. C. Jones, and C. Shearwood, *J. Infra-red Millimeter Waves* **14**, 1237 (1993).
- ¹³L. C. Ó Súilleabháin, H. P. Hughes, A. C. Churchill, D. A. Richie, M. P. Grimshaw, and G. A. C. Jones, *J. Appl. Phys.* **76**, 1701 (1994).
- ¹⁴J. Shah, A. Pinczuk, H. L. Strömer, A. C. Gossard, and W. Wiegmann, *Appl. Phys. Lett.* **42**, 322 (1984).
- ¹⁵F. F. Fang and A. B. Fowler, *J. Appl. Phys.* **41**, 1825 (1970).
- ¹⁶S. M. Goodnick and P. Lugli, *Phys. Rev. B* **37**, 2578 (1988).
- ¹⁷J. Shah and R. C. C. Leite, *Phys. Rev. Lett.* **22**, 1304 (1969).
- ¹⁸P. D. Southgate and D. S. Hall, *Appl. Phys. Lett.* **16**, 280 (1970).
- ¹⁹P. D. Southgate, D. S. Hall, and A. B. Dreeben, *J. Appl. Phys.* **42**, 2868 (1971).
- ²⁰C. Guillemot and F. Clérot, *Phys. Rev. B* **47**, 7227 (1993).
- ²¹M. Cardona, in *Light Scattering in Solids, II*, edited by M. Cardona and G. Guntherodt (Springer, Heidelberg, 1982), p. 32.
- ²²I. V. Kukushkin, K. von Klitzing, K. Ploog, and V. B.

- Timofeev, Phys. Rev. B **40**, 7788 (1989).
- ²³D. Richards, G. Fasol, and K. Ploog, Appl. Phys. Lett. **57**, 1099 (1990).
- ²⁴F. Stern, Phys. Rev. Lett. **18**, 546 (1967).
- ²⁵E. Batke, D. Heitmann, and C. W. Tu, Phys. Rev. B **34**, 6951 (1986).
- ²⁶R. Hiraoka and H. Sakaki, J. Appl. Phys. **63**, 803 (1985).
- ²⁷T. J. Drummond, M. Keerer, W. Kopp, H. Morkoc, K. Hess, and B. G. Streetman, Electron. Lett. **17**, 545 (1981).
- ²⁸Claude Weisbuch and Borge Vinter, *Quantum Semiconductor Structures: Fundamentals and Applications* (Academic, New York, 1991), p. 44.
- ²⁹J. P. Harrang, R. J. Higgins, R. K. Goodall, P. R. Jay, M. Laviro, and P. Delescluse, Phys. Rev. B **32**, 8126 (1985).
- ³⁰P. T. Coleridge, Phys. Rev. B **44**, 3793 (1991).
- ³¹F. F. Fang, T. P. Smith III, and S. L. Wright, Surf. Sci. **196**, 310 (1988).
- ³²S. Das Sarma and F. Stern, Phys. Rev. B **32**, 8442 (1985).
- ³³V. F. Sapega, V. I. Belitsky, T. Ruf, H. D. Fuchs, M. Cardona, and K. Ploog, Phys. Rev. B **46**, 16005 (1992).
- ³⁴I. V. Kukushkin, K. von Klitzing, and K. Ploog, Phys. Rev. B **37**, 8509 (1988).